The Astrophysical Journal, 674:L13–L16, 2008 February 10
© 2008. The American Astronomical Society. All rights reserved. Printed in U.S.A.

THE ENVIRONMENT OF GALAXIES AT LOW REDSHIFT

Nicolas B. Cowan[1] and Željko Ivezić[1]

Received 2007 November 8; accepted 2007 December 27; published 2008 January 10

ABSTRACT

We compare environmental effects in two analogous samples of galaxies, one from the Sloan Digital Sky Survey (SDSS) and the other from a semianalytic model (SAM) based on the Millennium Simulation (MS), to test to what extent current SAMs of galaxy formation are reproducing environmental effects. We estimate the large-scale environment of each galaxy using a Bayesian density estimator based on distances to all 10 nearest neighbors, and we compare broadband photometric properties of the two samples as a function of environment. The feedbacks implemented in the semianalytic model produce a qualitatively correct galaxy population with similar environmental dependence as that seen in SDSS galaxies. In detail, however, the colors of MS galaxies exhibit an exaggerated dependence on environment: the field contains too many blue galaxies, whereas clusters contain too many red galaxies, compared to the SDSS sample. We also find that the MS contains a population of highly clustered, relatively faint red galaxies with velocity dispersions comparable to their Hubble flow. Such high-density galaxies, if they exist, would be overlooked in any low-redshift survey, since their membership to a cluster cannot be determined because of the "fingers-of-God" effect.

Subject headings: galaxies: fundamental parameters — galaxies: luminosity function, mass function — galaxies: statistics

1. INTRODUCTION

Since the discovery of the morphology-environment relation (Dressler 1980), it has been known that galaxy properties are correlated with their large-scale environment: the average morphology, color, and luminosity of galaxies differ depending on how crowded their neighborhood is. On the face of it, it is not clear why or how the environment of a galaxy on megaparsec scales should be related to the kiloparsec-scale processes (star formation, supernova and active galactic nucleus [AGN] feedback) that determine the bulk properties of a galaxy. To further confuse matters, the strong correlation between morphology, color, and luminosity (Strateva et al. 2001 and references therein) makes it unclear which property is ultimately driven by environment let alone which physical processes are responsible. It is even possible that environmental effects are driven primarily by nature (different formation conditions) rather than nurture (galaxy-galaxy interactions). A critical step toward answering such questions is to compare observed trends to those present in a simulated galaxy ensemble, in which one knows all the processes at work.

The Sloan Digital Sky Survey (SDSS) is a powerful tool for addressing questions of environmental effects.[2] Its spectroscopic sample of galaxies is the largest such sample ever, ensuring that even relatively rare galaxy populations are well represented, and the survey's large contiguous footprint makes it easy to determine the large-scale environment for most of these galaxies. Previous researchers who have used the SDSS galaxy catalog to study environmental dependences have found three broad trends: (1) the peaks of the bimodal color distribution of galaxies do not shift for different environments; (2) blue and red galaxies are most common in low- and high-density environments, respectively; and (3) the luminosity of red galaxies increases with local density (Hogg et al. 2003; Kauffmann et al. 2004; Balogh et al. 2004; Tanaka et al. 2004; Blanton et al. 2005; Zehavi et al. 2005; Park et al. 2007; Ball et al. 2008).

The Millennium Simulation (MS; Springel et al. 2005) is the largest ever cosmological simulation, comprising some 10^{10} dark matter (DM) particles with a spatial resolution of 5 h_{100}^{-1} kpc. At $z = 0$, the simulation fills a cube 500 h_{100}^{-1} Mpc per side. The MS does not explicitly model the gas, dust, or stars that make up observable galaxies, but it produces a DM halo merger tree that serves as the backbone for a number of semianalytic models (SAMs). Unlike *N*-body/smoothed particle hydrodynamic simulations, SAMs do not simulate the gravitational and hydrodynamic forces involved in the formation and evolution of galaxies, but they do provide a computationally inexpensive way to explore the parameter space of subgrid processes. The trade-off is that the parameters of a SAM must be tuned using observations (e.g., matching to the observed luminosity function), making truly independent comparisons between the model and reality more challenging. Numerous groups have developed SAMs that hierarchically form some 10^7 galaxies from the MS merger tree (e.g., Croton et al. 2006; Bower et al. 2006; De Lucia & Blaizot 2007 and references therein). Their models differ—for example, in their treatment of AGN feedback—but all reproduce some of the empirical features of galaxy populations. The MS galaxies have a very realistic distribution of luminosities, thanks to judicious use of "radio" feedback. They also exhibit a bimodal color distribution, as discovered in the SDSS (Strateva et al. 2001). Finally, the power spectrum of the density fluctuations is in good agreement with the empirical data from the Two Degree Field Survey and the SDSS (Springel et al. 2005). Previous investigators have found that the brightest MS galaxies are red, dead ellipticals populating rich galaxy clusters (De Lucia et al. 2006), whereas the modeled galaxies in the very lowest density environments have similar colors and star formation rates as analogous SDSS galaxies (Patiri et al. 2006).

In this work, we compare the observed galaxy populations with those produced with SAMs. Our work differs from those listed above in the following ways: we use the Bayesian number density as a proxy for local environment, rather than the commonly used surface density or two-point correlation function; we use the $u - r$ color, which has more leverage than the

[1] Astronomy Department, University of Washington, Box 351580, Seattle, WA 98195; cowan@astro.washington.edu, ivezic@astro.washington.edu.

[2] Vizier Online Data Catalog, 2276 (J. K. Adelman-McCarthy et al., 2007).

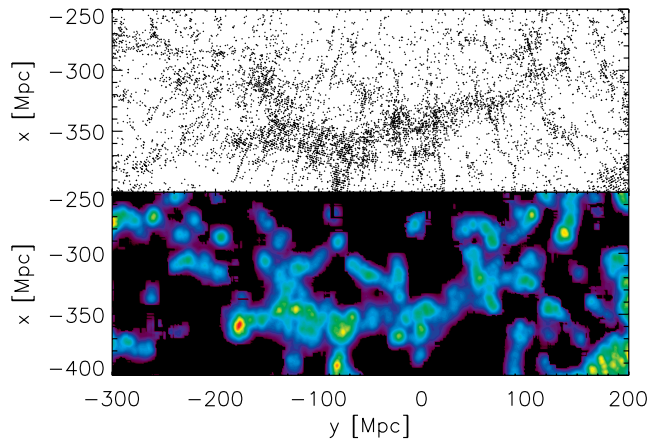

FIG. 1.—Map of the Sloan Great Wall, located on the celestial equator some 350 Mpc away from the Milky Way (see Fig. 9 in Gott et al. 2005). Due to the large distance to the purported structure, we applied a $M_r < -21$ cut to the DR5 galaxy catalog, yielding a sample of 129,974 galaxies complete to $z = 0.12$. The top panel shows the actual distribution of galaxies within $\pm 7°$ of the equatorial plane. The bottom panel shows a Bayesian density map with spatial resolution of 1 Mpc; the black areas correspond low-density environments, and the red regions denote the most massive clusters. This visualization resolves the wall into something more reminiscent of a mountain range.

$g - r$ color; we use SDSS Data Release 5, rather than any of the previous (smaller) releases; and, last but not least, we compare observed and modeled galaxies for the full range of galaxy environments and colors.

2. SELECTION CRITERIA

We use a sample of 674,749 galaxies from the SDSS Data Release 5 (DR5) main galaxy sample, which is an optical imaging and spectroscopic survey of galaxies over $\frac{1}{4}$ of the sky (with limiting magnitude $r < 17.7$ after foreground extinction removal). We create a complete volume- and luminosity-limited sample with $0.01 < z < 0.077$ (or distances of 43–345 Mpc from the Milky Way) and $M_r < -20$, leaving 90,689 galaxies. The characteristic galaxy luminosity in the SDSS r band is $M_* = -20.60$ (Blanton et al. 2003b), which falls well within our magnitude limit. We use model magnitudes corrected for foreground extinction but do not apply K-corrections (we instead apply K-corrections to the model galaxies); absolute magnitudes are computed using $h_0 = 0.732$ (Spergel et al. 2007). Because our sample of SDSS galaxies only extends to look-back times less than 1 Gyr, it is representative of local galaxies.

We use the modeled galaxies generated by De Lucia & Blaizot (2007) and available online through the Millennium Simulation database.[3] The quantities we use are the Cartesian positions and velocities of the galaxies, as well as their absolute SDSS u and r magnitudes, which include dust extinction from both a diffuse interstellar medium and an attenuation of stars in young clusters in the emitting galaxy (De Lucia et al. 2006). We make a $M_r < -20$ cut on the $z = 0$ snapshot, resulting in a complete sample of 1,805,780 galaxies in the simulation volume. We create a mock observational catalog for an observer at the origin by computing the right ascension, declination, and distance modulus of each galaxy. Since the model galaxies have rest-frame colors, we apply K-corrections using the model spectra of Bruzual & Charlot (2003), although this changes the colors by less than 0.2 mag. We then make cuts on radial distance, keeping only those galaxies that fall within the 43–345 Mpc range of our volume-limited SDSS sample. This mock "survey" covers one-eighth of the sky and contains 110,437 galaxies, ~20% more than our SDSS sample.

[3] See http://www.mpa-garching.mpg.de/millennium.

3. BAYESIAN DENSITY ESTIMATOR

The most common proxy for environment is the number density of galaxies, or the surface density of galaxies within redshift slices. For example, Blanton et al. (2005) use a deprojected angular correlation function, whereas Scoville et al. (2007) use an adaptively smoothed surface density. Other groups have used three-dimensional density estimators, such as the overdensity on a 8 h^{-1} Mpc scale (Hogg et al. 2003) or within a smoothing kernel (Park et al. 2007). Mateus et al. (2007) use a hybrid of three-dimensional and two-dimensional 10th nearest neighbor density, noting that the former tends to underestimate density in high-mass galaxy clusters. It is also common practice to use the three-dimensional galaxy correlation function as a metric for density (e.g., Zehavi et al. 2005), although it should be noted that the two-point correlation function is insensitive to higher order correlations that almost certainly exist between galaxies.

We compute densities using three-dimensional positions. Rather than use the traditional 10th nearest neighbor metric for number density, $N_{10} = 1/d_{10}^3$, we use a Bayesian metric (Ivezić et al. 2005):

$$n = C \frac{1}{\sum_{i=1}^{10} d_i^3}, \quad (1)$$

where $d_1 = 0$, if computing the density at the location of a galaxy. The constant $C = 11.48$ is empirically determined by demanding that $\langle n \rangle$ matches the actual number density when density is estimated on a regular grid for a uniform density field. As shown in Ivezić et al. (2005), the use of the distances to all 10 neighbors, as opposed to only the 10th neighbor, results in a factor of ~2 improvement in the precision of density estimates.

Although we are mostly interested in the density at the position of galaxies, the Bayesian density estimator can be used at arbitrary positions, allowing us to construct a density map on a regular grid. In Figure 1, we show the density map (with resolution 1 Mpc) for an equatorial slice of DR5, centered on the Sloan Great Wall of Gott et al. (2005). Thanks to the precision of our density estimator, it is easily discernible that the "wall" is not a monolithic structure but results from the juxtaposition of a collection of large clusters of galaxies.[4]

4. OBSERVATIONAL EFFECTS

Three observational effects that plague the SDSS galaxy sample could significantly affect the density distribution of galaxies: incompleteness, edge effects, and "fingers of God." In this section, we describe these effects and quantify how they influence the density distribution of SDSS galaxies.

For galaxies falling within 55″ of each other, only one galaxy gets a fiber, because of fiber collisions. Since 30% of the SDSS area consists of overlap regions between neighboring fields, the net effect of fiber collisions is a loss of 6% of the photometric galaxies that would otherwise be in the spectroscopic

[4] With the visualization shown in Fig. 1, this structure is more reminiscent of a mountain range than a great wall.

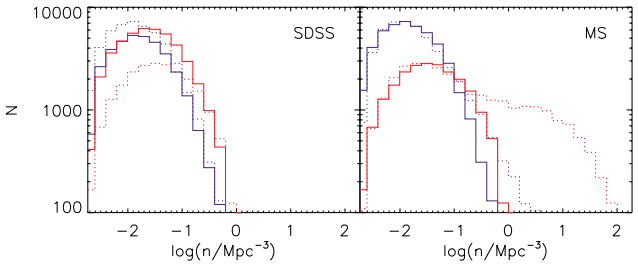

FIG. 2.—Local number density distribution for SDSS and MS galaxies in the left and right panels, respectively. The blue and red lines represent the density distribution for blue and red galaxies, based on a $u - r = 2.2$ cut. For reference, the dotted lines in the left panel show the distributions for blue and red MS galaxies (same as the solid lines in the right panel). The dotted lines in the right panel represent the density distribution of the MS before the application of observational effects.

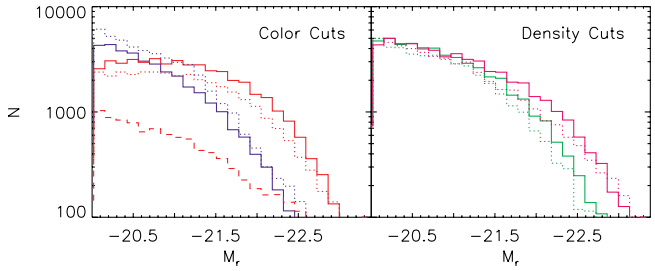

FIG. 3.—Luminosity function for SDSS (*solid lines*) and MS (*dotted lines*) galaxies divided by color in the left panel and by density in the right panel. Red and blue lines in the left panel represent the luminosity functions for red and blue galaxies, based on a $u - r = 2.2$ cut. The dashed line in the left panel shows the luminosity function of the MS galaxies with $n > 1$ Mpc^{-3} before the application of observational effects. Green and magenta lines in the right panel represent the luminosity function for the lowest and highest quartiles in density, respectively (normalized at the faint end).

catalog (Strauss et al. 2002). Fiber collisions notwithstanding, more than 95% of galaxies in the SDSS photometric catalog are given a fiber and are in the spectroscopic catalog. The bulk of the remaining 5% suffer from blending with saturated stars and do not significantly bias the spectroscopic galaxy sample (Strauss et al. 2002).

The tiling of SDSS fields is such that there are no gaps, except near the edges of the survey area (Blanton et al. 2003a). The density estimated near the edge of the DR5 footprint will be artificially low because SDSS spectra have not been obtained for many of the true nearest neighbors. To remove the most egregious offenders, we do not compute densities for any galaxies with fewer than 10 neighbors within a 10 Mpc radius or for galaxies falling within 10 Mpc of our redshift limits.

Galaxies in the SDSS spectroscopic catalog have small redshift uncertainties (30 km s^{-3}), but the true limiting factor for determining the radial distance to galaxies is the "fingers-of-God" effect: massive galaxy clusters have a large velocity dispersion, σ, which has the effect of smearing them out in redshift space and reducing their apparent density by a factor $1/(1 + \sigma/cz)$.

To quantify the impact of observational effects, we compare the density distribution for two versions of our mock survey of MS galaxies: one in which we model these effects and the other in which we do not. Fiber collisions are conservatively implemented by ignoring all neighbors within 55″ of a galaxy when computing density (this affects 6% of the galaxies, in good agreement with the estimate for SDSS fiber collisions). General spectroscopic incompleteness is implemented by removing 5% of the galaxies at random from the catalog. To increase the surface area–to–volume ratio—and hence the importance of edge effects—we limit our samples to galaxies lying *less than* 10 Mpc from a survey edge (reducing the size of the sample by a factor ~5). We model fingers of God by adding the peculiar velocity of each galaxy (obtained from the MS database) to its model Hubble flow and then computing its apparent radial distance from this mock redshift, rather than from its actual Cartesian position.

The density distributions for the mock MS survey with and without observational effects are shown as solid and dotted lines in the right panel of Figure 2. The distribution remains unaffected, except at high densities, where fingers of God completely erase the high-density tail (~3% of galaxies). If this extremely high density population of galaxies exists, it will only be detected in the next-generation surveys operating at higher redshifts, where the Hubble flow dominates over peculiar velocities. For the remainder of the Letter, we compare our SDSS galaxy sample to the mock MS survey, including the effects of fiber collisions, spectroscopic incompleteness, and "fingers of God."

5. ENVIRONMENT AND PHOTOMETRY OF GALAXIES

For the purposes of plotting our results, we remove outliers from both galaxy samples by cutting out the top and bottom percentile in color, as well as the top and bottom 0.1% in luminosity and density. The MS histograms are rescaled to the same total number of galaxies as for the SDSS. Figure 2 shows the density distributions for the SDSS and MS galaxies, separated into the blue and red mode based on the $u - r = 2.2$ cut of Strateva et al. (2001). (For comparison, the peak of the density distribution for random positions in the survey is $n = 10^{-2.8}$ Mpc^{-3} in either galaxy sample.) There are 50% too many blue galaxies in the MS as compared to the SDSS, despite the fact that the minimum in color for both samples occurs at $u - r = 2.2$ (see Fig. 4 below).

The luminosity functions for both sets of galaxies, shown in Figure 3, match very well, except for the overrepresentation of blue galaxies in the MS. The luminosity function of the very dense ($n > 1$ Mpc^{-3}) modeled galaxies—invisible in the mock survey—is shown with the dotted line in the left panel of Figure 3. These extremely high density environments are populated by relatively faint ($M_r > -21.5$) red galaxies, not luminous red galaxies. The luminosity function for the lowest and highest density quartiles, shown in the right panel of Figure 3, indicates that the SAM reproduces the environmental dependence of luminosity.

Figure 4 shows the color distribution for the lowest and highest density quartiles of each sample. The SDSS and MS galaxy samples both exhibit a bimodal color distribution with a minimum at $u - r = 2.2$, although the blue peak is too pronounced for MS galaxies. The peaks of the blue and red populations for the MS galaxies are approximately 0.2 mag too blue, as compared to the SDSS galaxies. In both panels, the relative heights of the red and blue peaks change as a function of density. Red galaxies represent $\sim\frac{2}{3}$ of the highest density quartiles of both the SDSS and MS samples. However, the environmental dependence of color is exaggerated for the lowest density quartile in the MS: 79% are blue, compared to only 52% for the SDSS sample (see also Patiri et al. 2006). The right panel of Figure 4 indicates that the SAM fails to reproduce

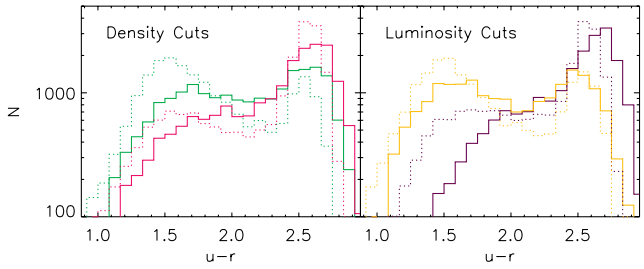

FIG. 4.—Color distribution for SDSS (*solid lines*) and MS (*dotted lines*) galaxies divided by density in the left panel and by luminosity in the right panel. Green and magenta lines in the left panel represent the color distribution for the lowest and highest quartiles in density, respectively. Yellow and purple lines in the right panel represent the luminosity function for the lowest and highest quartiles in luminosity, respectively.

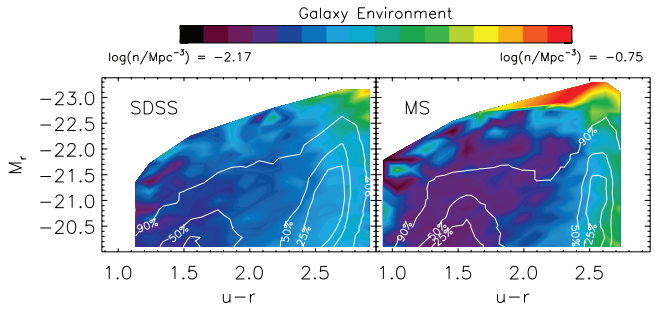

FIG. 5.—Color-magnitude diagram for SDSS and MS galaxies in the left and right panels, respectively. The labeled white lines show which regions on the plot are most populated (these are complete volume-limited samples), and the color-coded background shows the median local environment around galaxies with a given color and magnitude (dark corresponds to low densities; bright corresponds to high densities).

the dependence of color on luminosity, namely, that brighter red galaxies are redder.

All of the features and discrepancies described above can be qualitatively seen in Figure 5, which combines the color, luminosity, and density information for all the galaxies. The labeled white lines show which regions on the plot are most populated, and the color contours denote the median density of galaxies in a given color-magnitude bin. For galaxies less luminous than $M_r = -22$, $u - r$ color tracks density, whereas luminosity is independent of environment. For the brightest galaxies, however, density correlates with luminosity and not with color.

6. CONCLUSIONS

We have compared two analogous galaxy samples, one from the SDSS DR5 spectroscopic sample and one from the SAMs of De Lucia & Blaizot (2007) after correcting for the observational effects present in the former. The density distribution and the luminosity function of the modeled galaxies qualitatively match those for the SDSS sample, but there are 50% too many blue galaxies in the former. In detail, two additional discrepancies become apparent between the galaxy samples: MS galaxies are more blue in $u - r$ than are SDSS galaxies; the colors of galaxies depend more strongly on environment in the MS than in the SDSS. The strong environmental dependence manifests itself as an overrepresentation of blue galaxies overall and suggests that the feedbacks implemented by De Lucia & Blaizot (2007) exaggerate the role of galaxy environment. A population of relatively faint red galaxies in extremely high density environments is visible in the MS survey *without* observational effects. Such high-density environments would be imperceptible in the SDSS because of velocity dispersions comparable to the local Hubble flow.

N. B. C. is supported by the Natural Sciences and Engineering Research Council of Canada. The authors wish to thank G. Lemson for his help with MS queries as well as R. Roškar, D. Patton, and the anonymous referee for invaluable comments about this work. M. Jurić came up with the "mountain range" analogy. The Millennium Simulation was carried out by the Virgo Consortium at the Computing Center of the Max Planck Society in Garching. Funding for the SDSS and SDSS-II has been provided by the Alfred P. Sloan Foundation, the Participating Institutions, the National Science Foundation, the US Department of Energy, the National Aeronautics and Space Administration, the Japanese Monbukagakusho, the Max Planck Society, and the Higher Education Funding Council for England. The SDSS Web site is http://www.sdss.org/.

REFERENCES

Ball, N. M., Loveday, J., & Brunner, R. J. 2008, MNRAS, in press
Balogh, M. L., Baldry, I. K., Nichol, R., Miller, C., Bower, R., & Glazebrook, K. 2004, ApJ, 615, L101
Blanton, M. R., Eisenstein, D., Hogg, D. W., Schlegel, D. J., & Brinkmann, J. 2005, ApJ, 629, 143
Blanton, M. R., Lin, H., Lupton, R. H., Maley, F. M., Young, N., Zehavi, I. & Loveday, J. 2003a, AJ, 125, 2276
Blanton, M. R., et al. 2003b, ApJ, 592, 819
Bower, R. G., Benson, A. J., Malbon, R., Helly, J. C., Frenk, C. S., Baugh, C. M., Cole, S., & Lacey, C. G. 2006, MNRAS, 370, 645
Bruzual, G., & Charlot, S. 2003, MNRAS, 344, 1000
Croton, D. J., et al. 2006, MNRAS, 365, 11
De Lucia, G., & Blaizot, J. 2007, MNRAS, 375, 2
De Lucia, G., Springel, V., White, S. D. M., Croton, D., & Kauffmann, G. 2006, MNRAS, 366, 499
Dressler, A. 1980, ApJ, 236, 351
Gott, J. R., III, Jurić, M., Schlegel, D., Hoyle, F., Vogeley, M., Tegmark, M., Bahcall, N., & Brinkmann, J. 2005, ApJ, 624, 463
Hogg, D. W., et al. 2003, ApJ, 585, L5
Ivezić, Ž., Vivas, A. K., Lupton, R. H., & Zinn, R. 2005, AJ, 129, 1096
Kauffmann, G., White, S. D. M., Heckman, T. M., Ménard, B., Brinchmann, J., Charlot, S., Tremonti, C., & Brinkmann, J. 2004, MNRAS, 353, 713
Mateus, A., Sodré, L., Cid Fernandes, R., & Stasińska, G. 2007, MNRAS, 374, 1457
Park, C., Choi, Y.-Y., Vogeley, M. S., Gott, J. R. I., & Blanton, M. R. 2007, ApJ, 658, 898
Patiri, S. G., Prada, F., Holtzman, J., Klypin, A., & Betancort-Rijo, J. 2006, MNRAS, 372, 1710
Scoville, N., et al. 2007, ApJS, 172, 150
Spergel, D. N., et al. 2007, ApJS, 170, 377
Springel, V., et al. 2005, Nature, 435, 629
Strateva, I., et al. 2001, AJ, 122, 1861
Strauss, M. A., et al. 2002, AJ, 124, 1810
Tanaka, M., Goto, T., Okamura, S., Shimasaku, K., & Brinkmann, J. 2004, AJ, 128, 2677
Zehavi, I., et al. 2005, ApJ, 630, 1